Off-centre convective zones in post-mass transfer stellar models

A. Miszuda

Nicolaus Copernicus Astronomical Centre, Polish Academy of Sciences, Bartycka 18, PL 00-716 Warsaw, Poland
e-mail: amiszuda@camk.edu.pl, miszuda.amadeusz.astronomy@gmail.com

ABSTRACT

We report the physical origin of transient off-centre convective zones (oCZs) that arise in mass accreting stellar models. Using detailed MESA simulations of binary evolution, we find that these oCZs are not numerical artefacts but emerge due to a local increase in density near the retreating edge of the convective core. The density enhancement raises the local opacity, which amplifies the radiative temperature gradient ∇_{rad}. If this gradient surpasses the Ledoux threshold ∇_{L}, defined by both thermal and compositional stratification, the region becomes convectively unstable. The resulting oCZs are detached from the convective core and transient: mixing within the oCZ erases the local gradient in mean molecular weight, leaving a sharp ∇_μ discontinuity at the boundary, stabilizing the adjacent layers. This mechanism naturally explains the presence and evolution of oCZs, as previously reported in massive interacting stars.

Key words. stars: evolution – stars: interiors – stars: binaries: close – convection

1. Introduction

In binary stellar evolution, mass transfer episodes strongly modify the internal structure of the accretor and donor stars. This structural reconfiguration is particularly complex near the end of Roche-lobe overflow (RLOF), where convective boundaries often shift, mix, or even split. A specific feature seen in stellar evolution models after mass accretion is the presence of convective zones that are located above the convective core, disconnected from it. These so-called off-centre convective zones (oCZs) have been reported in binary models by Renzo & Götberg (2021), but their physical origin remained unexplained. Subsequent studies also showed that oCZs significantly modify the internal structure of post-interaction stars (e.g., see Figure 3 of Wagg et al. 2024), yet no physical mechanism has been proposed to account for their formation.

In this Letter, we present a physical mechanism responsible for the formation of oCZs. We show that in binary models of the mass accreting star, mass accretion and enhanced mixing near the convective core retreating boundary create a narrow region with a local bump in density (as compared to the same mass single-star model equivalent, opposed to Renzo & Götberg 2021, where they observe a local drop). This leads to an increase in the local opacity, which, in turn, causes a peak in the radiative temperature gradient, ∇_{rad}. When ∇_{rad} exceeds the Ledoux temperature gradient, ∇_{L}, it violates the Ledoux criterion for stability and convection is temporarily triggered in a thin off-centre shell. These zones are transient, as mixing rapidly washes-out any local mean molecular weight gradients, ∇_μ, thereby reducing ∇_{L} and restoring convective stability. Our results explain the structure and time evolution of these oCZs.

2. Methods

We use the MESA stellar evolution code (version r23.05.1; Paxton et al. 2011, 2013, 2015, 2018, 2019; Jermyn et al. 2023) to compute non-rotating binary evolution models for system undergoing stable mass transfer. The models consist of a binary system with initially $10\,\mathrm{M}_\odot$ primary and a $7\,\mathrm{M}_\odot$ secondary in a circular orbit with a period of 3 days. The binary is evolved through conservative mass transfer until the accretor star reaches 10 $\mathrm{M}_\odot$. For subsequent evolution, we assume the accretor evolves as a single, isolated star until central hydrogen exhaustion.

In our evolutionary computations, we adopted Asplund et al. (2009) initial chemical composition and used the OPAL opacity tables, supplemented by data from Ferguson et al. (2005) for lower temperatures. For high-temperature regimes, as well as hydrogen-poor or metal-rich conditions, we used CO enhanced tables. We assumed a metallicity of $Z = 0.014$ (Nieva & Przybilla 2012) and an initial hydrogen abundance of $X_0 = 0.723$, using scaling relations as in Choi et al. (2016).

Convective mixing is treated with the Ledoux criterion, combined with time-dependent convection following the formalism of Kuhfuss (1986), with a mixing-length parameter $\alpha_{\mathrm{MLT}} = 0.5$. Semiconvective mixing is included according to the prescription of Langer et al. (1985), adopting $\alpha_{\mathrm{sc}} = 0.1$. Thermohaline mixing is implemented following Kippenhahn et al. (1980), with an efficiency parameter $\alpha_{\mathrm{th}} = 1$. Convective overshooting above the hydrogen-burning core is treated using an exponentially decaying diffusion scheme (Herwig 2000), with an overshooting parameter $f_{\mathrm{ov}} = 0.02$ (Johnston et al. 2024). As our models did not include rotational mixing, we introduced a minimum diffusive mixing coefficient of $D = 100\ \mathrm{cm^2\,s^{-1}}$ to smooth out numerical noise or discontinuities in internal profiles.

We explore the numerical stability of our results against changes in both spatial and time step resolution, testing various configurations and ultimately adopting `mesh_delta_coeff = 0.2` and `time_delta_coeff = 0.5`.

3. Results

Off-centre convective zones systematically appear in our models of the mass accreting star during the late stages of RLOF.
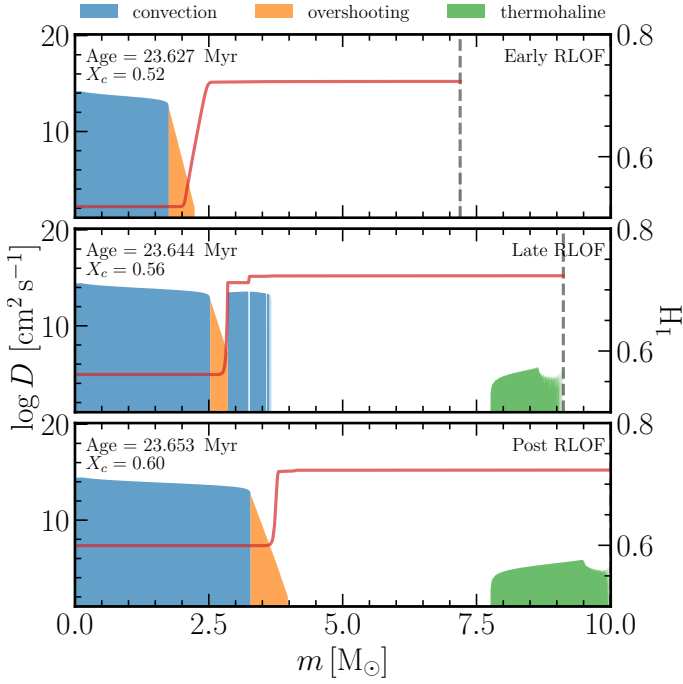
Fig. 1. Internal mixing profiles and hydrogen abundance distributions (red lines) for three evolutionary stages: early, late, and post mass transfer. Coloured regions correspond to different mixing processes, including convection, overshooting, and thermohaline mixing, as labelled. The red solid lines show the internal hydrogen profiles, and the dashed vertical lines show current stellar mass.

Their development is illustrated in Figure 1, which shows the internal mixing structure at three evolutionary stages: early, late, and post-accretion. Each panel presents diffusion coefficients associated with convection, overshooting, and thermohaline mixing. The current stellar mass of the accretor is marked by dashed vertical lines. The red curves trace the hydrogen distribution inside the star, capturing the impact of successive mixing episodes. Rejuvenation of the stellar core is evident across the sequence, indicated by the increasing central hydrogen abundance and the expansion of the convective core. Notably, during the late RLOF phase, multiple detached oCZs emerge. These zones are chemically homogeneous, with nearly constant hydrogen abundance, while steep hydrogen gradients appear in the narrow regions separating them.

According to the Ledoux criterion (Ledoux 1947), the onset of convection depends not only on the temperature stratification but also includes stabilising effects from composition gradients:

$$\nabla_{\rm rad} > \nabla_{\rm L}, \text{ where } \nabla_{\rm L} = \nabla_{\rm ad} + \frac{\varphi}{\delta}\nabla_\mu.$$

Here, $\nabla_{\rm rad}$ is the radiative temperature gradient and $\nabla_{\rm L}$ is the Ledoux gradient composed with $\nabla_{\rm ad}$, the adiabatic gradient, and $\nabla_\mu = {\rm d}\ln\mu/{\rm d}\ln P$, the gradient of the mean molecular weight. The coefficients $\delta = -\left(\frac{\partial\ln\rho}{\partial\ln T}\right)_{P,\mu}$ and $\varphi = \left(\frac{\partial\ln\rho}{\partial\ln\mu}\right)_{P,T}$ are thermodynamic derivatives obtained from the equation of state (e.g., Kippenhahn & Weigert 1990). When the inequality is satisfied, the stratification becomes dynamically unstable and convection is initiated, even in the presence of stabilising composition gradients.

The internal profiles of $\nabla_{\rm rad}$ and $\nabla_{\rm L}$ for models close to those shown in Figure 1 (compare the ages and core-hydrogen abundances) are presented in Figure 2, indicated by blue and orange

lines, respectively. The right-hand ordinates display the corresponding profiles of opacity κ (red), density $\log\rho$ (brown), and hydrogen abundance ^{1}H (grey lines), plotted in the inner $5\,{\rm M}_\odot$ of the mass coordinate. The shaded regions mark the convectively unstable layers, where $\nabla_{\rm rad} > \nabla_{\rm L}$.

As the accretor grows in mass, a density glitch develops and $\nabla_{\rm rad}$ locally increases within the chemically stratified region left behind by the previously retreating convective core. When $\nabla_{\rm rad}$ exceeds $\nabla_{\rm L}$, the Ledoux stability criterion is violated, and convection is triggered in a narrow shell. This convection rapidly homogenizes the chemical composition within the shell. However, since the surrounding layers retain steep ∇_μ profiles, mixing leads to sharp discontinuities in composition and density at the boundaries (most visible in the middle panel of Figure 2). These discontinuities produce strong chemical gradients that locally exceed $\nabla_{\rm rad}$, thereby segmenting the oCZs.

The rise in $\nabla_{\rm rad}$ can be traced to structural adjustments at the core-envelope boundary following mass accretion. As fresh material is deposited onto the gainer, the convective core responds by expanding and partially mixing with the surrounding envelope. This convective boundary mixing process supplies fresh hydrogen to the core and facilitates stellar rejuvenation (e.g., Neo et al. 1977; Renzo et al. 2023). Although a strong Ledoux gradient develops in this region due to the composition discontinuity, it does not directly increase $\nabla_{\rm rad}$. However, the associated density jump and abrupt increase in hydrogen content ^{1}H lead to a local enhancement in the Rosseland mean opacity, κ. This, in turn, raises the radiative temperature gradient according to

$$\nabla_{\rm rad} \propto \frac{\kappa L P}{m T^4}.$$

The increased opacity thus plays a central role in initiating off-centre convection. In this region, where $\log T \approx 7.3 - 7.4$, the opacity rise is primarily driven by bound-free and free-free transitions, which are highly sensitive to both density and hydrogen content, thereby amplifying the opacity response to structural perturbations. Rather than the density change itself, it is the structural response to mass accretion — specifically the interplay between density and composition — that governs the local instability.

4. Discussion

Our models provide a self-consistent physical explanation for the emergence of off-centre convective zones in mass-accreting stars. These regions form as a result of structural changes accompanying the stellar mass growth. Specifically, the development of a narrow, higher-density layer within the chemically stratified zone left behind by the receding convective core leads to a local increase in opacity and, consequently, a rise in the radiative temperature gradient. This configuration arises naturally from the interior's response to continued accretion and convective boundary mixing.

We confirm that the oCZs are not numerical artefacts. Their presence persists across models computed with different time resolutions and mesh settings, and their properties remain consistent. The zones vanish once convective mixing within the oCZs reduces the local density gradient in the stratified region, supporting the conclusion that both their formation and disappearance are governed by physical, rather than numerical, processes.

These transient convective regions may have several implications. They modify the local μ-profile, which can influence the
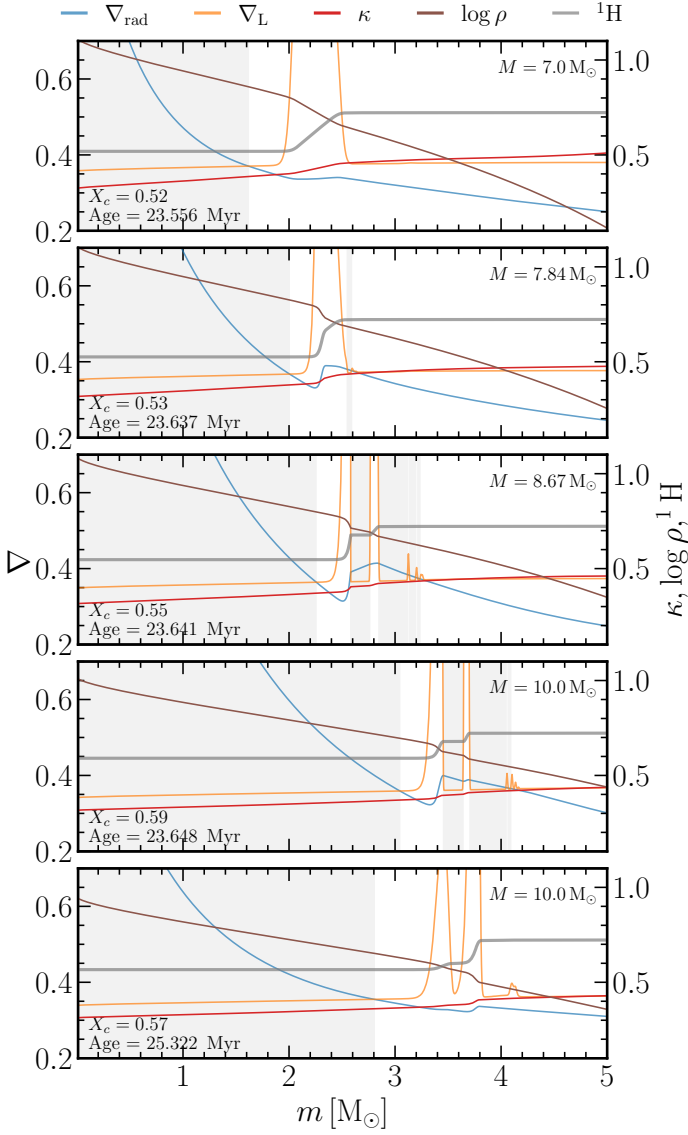
Fig. 2. Temperature gradients and structural profiles in representative models before, during and after mass transfer. Shaded areas indicate convectively unstable zones.

behaviour of buoyancy- (Wagg et al. 2024; Henneco et al. 2024, 2025) and pressure-modes (Miszuda 2025, Miszuda et al., in prep.) in post-interaction stars. While they do not significantly contribute to core rejuvenation, in certain configurations they may facilitate it by enhancing the transport of hydrogen into the central regions. They could also affect the timescales and spatial extent of subsequent mixing episodes. Whether similar structures form in rotating, mass accreting stars remains to be explored.

5. Conclusions

We identify a robust physical mechanism for the formation of off-centre convective zones in mass-accreting stellar models. These zones arise from local density enhancements that increase the Rosseland mean opacity and, in turn, the radiative gradient. Once ∇_{rad} exceeds the Ledoux threshold, convection sets in within a narrow shell. Continued mixing within this region gradually smooths the local density and composition gradients,

eventually suppressing the instability and restoring radiative stability.

This mechanism is repeatable and independent of numerical choices. It explains transient convective features observed in mass-accreting stellar models and highlights the importance of resolving fine-scale mixing structures. These results have implications for binary evolution, internal mixing, and the interpretation of g- and p-mode pulsations in post-interaction systems.

Software

MESA (Paxton et al. 2011, 2013, 2015, 2018, 2019; Jermyn et al. 2023),
PYMESAREADER (https://billwolf.space/py_mesa_reader/index.html),
PYTHON SCIPY (Virtanen et al. 2020)

References

Asplund, M., Grevesse, N., Sauval, A. J., & Scott, P. 2009, ARA&A, 47, 481
Choi, J., Dotter, A., Conroy, C., et al. 2016, ApJ, 823, 102
Ferguson, J. W., Alexander, D. R., Allard, F., et al. 2005, ApJ, 623, 585
Henneco, J., Schneider, F. R. N., Hekker, S., & Aerts, C. 2024, A&A, 690, A65
Henneco, J., Schneider, F. R. N., Heller, M., Hekker, S., & Aerts, C. 2025, arXiv e-prints, arXiv:2504.08683
Herwig, F. 2000, A&A, 360, 952
Jermyn, A. S., Bauer, E. B., Schwab, J., et al. 2023, ApJS, 265, 15
Johnston, C., Michielsen, M., Anders, E. H., et al. 2024, ApJ, 964, 170
Kippenhahn, R., Ruschenplatt, G., & Thomas, H. C. 1980, A&A, 91, 175
Kippenhahn, R. & Weigert, A. 1990, Stellar Structure and Evolution (Springer-Verlag)
Kuhfuss, R. 1986, A&A, 160, 116
Langer, N., El Eid, M. F., & Fricke, K. J. 1985, A&A, 145, 179
Ledoux, P. 1947, ApJ, 105, 305
Miszuda, A. 2025, arXiv e-prints, arXiv:2502.10493
Neo, S., Miyaji, S., Nomoto, K., & Sugimoto, D. 1977, PASJ, 29, 249
Nieva, M. F. & Przybilla, N. 2012, A&A, 539, A143
Paxton, B., Bildsten, L., Dotter, A., et al. 2011, ApJS, 192, 3
Paxton, B., Cantiello, M., Arras, P., et al. 2013, ApJS, 208, 4
Paxton, B., Marchant, P., Schwab, J., et al. 2015, ApJS, 220, 15
Paxton, B., Schwab, J., Bauer, E. B., et al. 2018, ApJS, 234, 34
Paxton, B., Smolec, R., Schwab, J., et al. 2019, ApJS, 243, 10
Renzo, M. & Götberg, Y. 2021, ApJ, 923, 277
Renzo, M., Zapartas, E., Justham, S., et al. 2023, ApJ, 942, L32
Virtanen, P., Gommers, R., Oliphant, T. E., et al. 2020, Nature Methods, 17, 261
Wagg, T., Johnston, C., Bellinger, E. P., et al. 2024, A&A, 687, A222